

# Seeking the Ultraviolet Ionizing Background at $z \approx 3$ with the Keck Telescope

Andrew J. Bunker<sup>1</sup>, Francine R. Marleau & James R. Graham

Astronomy Department, 601 Campbell Hall, University of California, Berkeley CA 94720

email: bunker@bigz.Berkeley.EDU

## ABSTRACT

We describe the initial results of a deep long-slit emission line search for redshifted ( $2.7 < z < 4.1$ ) Ly $\alpha$ . These observations are used to constrain the fluorescent Ly $\alpha$  emission from the population of clouds whose absorption produces the higher-column-density component of the Ly $\alpha$  forest in quasar spectra. We use the results to set an upper limit on the ultraviolet ionizing background. Our spectroscopic data obtained with the Keck II telescope at  $\lambda/\Delta\lambda_{\text{FWHM}} \approx 2000$  reveals no candidate Ly $\alpha$  emission over the wavelength range of 4500–6200 Å along a 3' slit in a 5400 s integration. This null result places the strongest limit to date on the ambient flux of Lyman continuum photons at  $z \approx 3$ . Typically we attain a  $1 \sigma$  surface brightness sensitivity to spectrally unresolved line emission in a  $1 \square''$  aperture of  $(0.4\text{--}0.6) \times 10^{-18} \text{ erg s}^{-1} \text{ cm}^{-2} \text{ arcsec}^{-2}$ , and we search for extended emission over a wide range of spatial scales. Our  $3 \sigma$  upper bound on the mean intensity of the ionizing background at the Lyman limit is  $J_{\nu 0} < 2 \times 10^{-21} \text{ erg s}^{-1} \text{ cm}^{-2} \text{ Hz}^{-1} \text{ sr}^{-1}$  for  $2.7 < z < 3.1$  (where we are most sensitive), assuming Lyman limit systems have typical radii of 70 kpc ( $q_0 = 0.5$ ,  $H_0 = 50 \text{ km s}^{-1} \text{ Mpc}^{-1}$ ). This constraint is more than an order of magnitude more stringent than any previously published direct limit. However, it is still a factor of three above the ultraviolet background level expected due to the integrated light of known quasars at  $z \approx 3$ . This pilot study confirms the conclusion of Gould & Weinberg (1996) that integrations of several hours on a 10-m class telescope should be capable of measuring  $J_{\nu 0}$  at high redshift. Our results suggest that the integrated flux of Lyman continuum photons escaping from star-forming galaxies at these epochs cannot exceed twice that from known quasars, and that the completeness of optically-selected quasar catalogues must be better than 30%. We also show that it is unlikely that decaying relic neutrinos, if comprising the bulk of the dark matter, are responsible for the meta-galactic radiation field.

---

<sup>1</sup>NICMOS Postdoctoral Researcher

*Subject headings:* quasars: absorption lines — intergalactic medium — galaxies: starburst — quasars: individual PKS0528-250 — diffuse radiation — early Universe

## 1. Introduction

In most models of structure formation the majority of baryonic matter in the Universe is contained in a uniformly-distributed intergalactic medium (IGM), which is predicted as a product of primordial nucleosynthesis. The Gunn-Peterson constraint on the H I component of this IGM (Gunn & Peterson 1965; Scheuer 1965) implies that the gas must have been highly ionized by  $z \sim 5$ , because the flux decrement observed on the blue side of the Ly $\alpha$  emission lines in the spectra of high-redshift quasi-stellar objects (QSOs) appears to be entirely consistent with absorption by discrete clouds along the line of sight (Steidel & Sargent 1987; Giallongo *et al.* 1994).

The meta-galactic ultraviolet (UV) background, which is widely believed to be primarily the integrated light of QSOs, is thought to be responsible for maintaining the diffuse IGM and the Ly $\alpha$  forest clouds in a highly-ionized state. This UV background may also be responsible for the ionization of metal-rich QSO absorption systems (Steidel 1990), the ionization of H I clouds in the Galactic halo (Ferrara & Field 1994), as well as for producing the sharp edges of H I disks in nearby spirals (Dove & Shull 1994; Maloney 1993; Bland-Hawthorn, Freeman & Quinn 1997).

From the evolution of the QSO luminosity function, recent theoretical calculations for  $z \approx 2.5$ –3 indicate that the contribution of observed QSOs alone to the mean intensity of the UV background is  $J_{\nu 0(-21)} \approx 0.6$  at the Lyman limit, i.e., at a frequency  $\nu_0 = c / 912 \text{ \AA}$  (Haardt & Madau 1996, hereafter HM96). Throughout we adopt the notation  $J_{\nu 0(-21)} = J_{\nu 0} / 10^{-21} \text{ erg s}^{-1} \text{ cm}^{-2} \text{ Hz}^{-1} \text{ sr}^{-1}$  and we assume a cosmology of  $q_0 = 0.5$ ,  $\Lambda_0 = 0$  and  $h_{50} = H_0 / 50 \text{ km s}^{-1} \text{ Mpc}^{-1}$ , unless otherwise stated. Indirect estimates of  $J_{\nu 0}$  are uncertain (see §3) and, given its importance, strenuous efforts have been made to directly measure the meta-galactic UV background. Hogan & Weymann (1987) proposed that long-slit spectroscopy of “blank sky” should reveal patches of fluorescent Ly $\alpha$  emission from Ly $\alpha$  forest clouds excited by the meta-galactic background. A detailed radiative-transfer treatment of Ly $\alpha$  emission from thick clouds ( $N_{\text{HI}} > 10^{20} \text{ cm}^{-2}$ ) photo-ionized by the meta-galactic radiation is given by Binette *et al.* (1993).

In a more recent paper, Gould & Weinberg (1996) show that for clouds with column

density  $N_{\text{HI}} \gtrsim 3 \times 10^{18} \text{ cm}^{-2}$  (optically thick to Lyman continuum photons),  $\simeq 50\%$  of the incident energy of the ionizing background emerges in the form of Ly $\alpha$  photons, including those resulting from collisional excitation. This fraction is robust and independent of cloud geometry, implying uniform surface brightness. A Ly $\alpha$  photon is absorbed and re-emitted within the cloud until it is Doppler shifted by an atom with a velocity  $\pm 4 \sigma_v$ , at which point it can escape. A cloud with a typical one-dimensional (1D) velocity dispersion of  $\sigma_v = 30 \text{ km s}^{-1}$  would have a double-peaked Ly $\alpha$  line with a separation of  $8 \sigma_v = 240 \text{ km s}^{-1}$ . Hence, moderate-resolution spectroscopy ( $R = \lambda/\Delta\lambda_{\text{FWHM}} \simeq 1500$ ) of an optically-thick cloud, along with adequate integration time, will yield a direct measurement of the intensity of the ionizing background. Lowenthal *et al.* (1990) have observed the Lyman limit system (LLS) towards Q0731+653, and on the basis of a two hour exposure spectrogram with the Multiple Mirror Telescope (MMT), place a  $2 \sigma$  upper limit of  $J_{\nu 0(-21)} < 200$  at  $z = 2.91$ , on the assumption that the clouds are only  $1''$  in extent. Comparable sensitivity is obtained by Martínez-González *et al.* (1995) through narrow-band imaging on the Isaac Newton Telescope (INT). Assuming larger clouds ( $\sim 10''$ ), their  $3 \sigma$  upper-limit is equivalent to  $J_{\nu 0(-21)} < 80$  at  $z = 3.4$  (see Figure 1 and Equation 2).

Moderate-dispersion long-slit spectroscopy appears the most promising technique with which to detect Ly $\alpha$  fluorescence. From typical quasar lines-of-sight, there are on average one or more optically-thick LLS per unit redshift interval at  $z > 2$  (Stengler-Larrea *et al.* 1995). Hence, a single spectrogram with a slit a few arcmin in length will intercept several such high-column-density clouds (see §2.3). Imaging with narrow-band interference filters (typically  $R \approx 100$ ), although covering a larger solid angle over a smaller redshift interval, provides less contrast against the sky for line emission than does spectroscopy. Therefore, narrow-band imaging cannot achieve the required sensitivity without prohibitively long integrations. Similarly, the expected surface brightness of Ly $\alpha$  is at least an order of magnitude too faint to be detected in the deepest broad-band optical imaging, i.e., the Hubble Deep Field (Williams *et al.* 1996). Even if sufficient depth could be attained, since the broad-band covers a large slice of redshift space the measurement would be confusion limited, as the LLS clouds (expected to be  $\sim 10''$  in extent, §2.3) would overlap.

In this paper, we present the results of deep Keck II long-slit spectroscopy with the Low Resolution Imaging Spectrometer (LRIS, Oke *et al.* 1995) at moderately-high dispersion in the blue,  $150 \text{ km s}^{-1}$  full width half maximum (FWHM). In §2 we describe the long-slit spectroscopic observations obtained, detail the data reduction procedures and determine an upper-limit to  $J_{\nu 0}$ . We discuss the cosmological implications in §3.

## 2. Observations

As part of another program, we have been undertaking deep long-slit spectroscopy on the fields of QSOs whose spectra show damped Ly $\alpha$  absorption systems. One field involved a set-up in the blue with a high-dispersion grating, and we are able to use the “blank sky” in the long-slit spectrogram for this investigation. The primary targets in these data are two actively star-forming galaxies at  $z = 2.81$  (S2 & S3 in Warren & Møller 1996) with angular separations of  $12''$  &  $21''$  from the  $z_{\text{em}} \approx z_{\text{abs}}$  QSO/damped system PKS0528–250, which lies at the same redshift. The coordinates of the slit center were  $\alpha_{2000} = 05^{\text{h}}30^{\text{m}}09^{\text{s}}.35$ ,  $\delta_{2000} = -25^{\circ}03'28''.2$ , and the position angle was set to  $95.2$  East of North so as to intercept both galaxies. The spectra of the target objects are to be presented in a forthcoming paper (Bunker *et al.* 1998).

We obtained the long-slit spectroscopy on the night of 1998 January 20 U.T. using LRIS at the f/15 Cassegrain focus of the 10-m Keck II Telescope. The LRIS detector is a Tek 2048<sup>2</sup> CCD with  $24 \mu\text{m}$  pixels and an angular scale of  $0''.212$  per pixel. We read out the CCD in two-amplifier mode. The observations were obtained using the 900 line  $\text{mm}^{-1}$  grating in first order blazed at  $5500 \text{ \AA}$ , producing a dispersion of  $0.839 \text{ \AA}$  per pixel. The reference arc lamps and sky-lines have  $\text{FWHM} \approx 3\text{--}3.5$  pixels, so for objects that fill the slit, the velocity width of a spectrally unresolved line is  $\text{FWHM} \approx 150\text{--}175 \text{ km s}^{-1}$ . The grating was tilted to sample the wavelength range  $4500\text{--}6200 \text{ \AA}$ , corresponding to Ly $\alpha$  in the redshift range  $2.7 < z < 4.1$ . The observations used the  $1''$  by  $3'$  long-slit. A total of 5400 s of on-source integration was obtained, and this was broken into three individual exposures of duration 1800 s that spanned an airmass range of 1.41–1.53. The telescope was dithered by  $7''.5$  along the slit between each integration to enable more effective cosmic ray rejection and the elimination of bad pixels. In the  $B$ -band the seeing had a  $\text{FWHM} = 0''.8\text{--}1''.1$ , and the sky background (no moon) was  $22.3 \text{ mag arcsec}^{-2}$ .

Spectrophotometric standard stars G191B2B & HZ44 (Massey *et al.* 1988; Massey & Gronwall 1990) were observed at similar airmass to determine the spectral shape of the sensitivity function, but our observations were rendered non-photometric by intermittent thin cirrus. However, we were able to boot-strap our spectrophotometry to the narrow-band Ly $\alpha$  line fluxes from Møller & Warren (1993) of the two  $z = 2.81$  star-forming galaxies on the long slit. As we expect the Ly $\alpha$  emitting patches to have dimensions much greater than our slit width and to have approximately uniform surface brightness, the photometric zero-points were corrected for slit losses using standard star observations with two different slit widths.

## 2.1. Data Reduction

The initial stages of the data reduction followed standard procedures and were accomplished using IRAF<sup>2</sup>. All the calibration and data frames were bias subtracted by fitting a low-order function to the appropriate over-scan region. Each half of the CCD was then converted to photo-electrons by correcting for the gain of the corresponding read-out amplifier. A high signal-to-noise ratio (SNR) dark frame was then subtracted.

The next step consisted of calibrating the pixel-to-pixel sensitivity variations of the CCD. Contemporaneous flat fields were obtained with a halogen lamp immediately after the science exposures, and these internal flats were normalized through division by the extracted lamp spectrum. The SNR for these flat fields was 100–300 per pixel. In order to remove the residual lower spatial frequency variations in the flat field due to non-uniform illumination of the slit, we also obtained spectral dome and twilight-sky flats. Cosmic rays were identified in the flat fielded spectra by iteratively calculating the noise in each column perpendicular to the dispersion axis and identifying discrepant pixels; those pixels associated with structure sharper than the point-spread function (PSF) were flagged as cosmic rays.

Wavelength calibration was obtained from arc lamp spectra also taken immediately after the data frames. To quantify the distortions across the CCD, we traced the centroid of each arc-line (and the sky-lines in the data frames) at 10 pixel intervals over the length of the slit (800 pixels). It was found that the centroids of the lines shifted by up to 3 pixels, comparable to the instrumental resolution. This distortion was well fit by a quadratic along the columns (the spatial axis) and a cubic along the rows (the dispersion direction). Hence we were able to form a distortion matrix to map from a pixel space to a wavelength solution, leaving RMS residuals to the fit of 0.1 pixels (0.08 Å).

Rather than doing the sky-subtraction in the usual manner by fitting a polynomial to each column (which might subtract the extended emission we are looking for), we first rectified the sky lines using the distortion matrix. We then created a high SNR 1D sky spectrum by averaging the rectified rows. The slit illumination function was determined by collapsing the two-dimensional (2D) blank sky spectrum dispersion axis, and this function was used to scale the 1D sky spectrum for row-by-row sky subtraction.

The individual sky-subtracted, rectified 2D spectra taken at different dither positions

---

<sup>2</sup>The Image Reduction and Analysis Facility (IRAF) is distributed by the National Optical Astronomy Observatories, which are operated by the Association of Universities for Research in Astronomy, Inc., under cooperative agreement with the National Science Foundation.

along the slit were then registered and averaged, with a percentile clipping algorithm used to reject cosmic rays that had escaped previous cuts. A mask was used to flag the known bad pixels, which were excluded from the averaging. The individual 1800 s integrations were sufficiently long for our data to be background (rather than read-out noise) limited at all wavelengths. The measured noise agreed well with the Poissonian statistics of the sky background, demonstrating that any additional noise introduced by our data reduction techniques was insignificant.

## 2.2. Analysis

After rectification and sky-subtraction, we searched for extended Ly $\alpha$  line emission by applying various filters along the spatial axis of the combined 2D spectrum. We convolved the 2D spectrum with a highly-elliptical 2D Gaussian oriented parallel to the slit. For the minor axis (along the dispersion direction), the width of the kernel was set to be comparable to the spectral resolution. We varied the length of the major axis to search for signal on any characteristic scale length between 1'' (our seeing disk) and 180'' (the length of the slit). For the anticipated range in  $J_{\nu 0}$ , the signal per resolution element is not large, so this smoothing is essential. We repeated the smoothing with simple boxcar filtering of various lengths along the slit axis, followed by convolution with a Gaussian of comparable extent to the seeing disk. This second approach is optimal if the Ly $\alpha$  clouds do indeed have uniform surface brightness (Gould & Weinberg 1996). For both techniques, visual inspection revealed no significant extended single-line emission.

The only Ly $\alpha$  line-emission sources detected were the target galaxies, PKS0528–250 S1 & S2. These have also been observed in continuum imaging (Møller & Warren 1998), with rest-frame equivalent widths of  $W_0 = 88 \text{ \AA}$  &  $46 \text{ \AA}$  respectively. This implies that Ly $\alpha$  arises from an internal UV source (star formation or AGN activity). Charlot & Fall (1993) calculate  $W_0 = 80\text{--}200 \text{ \AA}$  for a star forming galaxy, depending on the initial mass function (IMF). However, selective extinction of this line through resonant scattering and suppression by dust can greatly reduce the equivalent width of Ly $\alpha$  in star forming galaxies (e.g., Steidel *et al.* 1996). In stark contrast, Ly $\alpha$  produced by external photo-ionization should have a much larger equivalent width, as the continuum arises mainly from two-photon decays. Hence, the rest-UV continuum around Ly $\alpha$  provides excellent discrimination between local OB stars and the diffuse meta-galactic background as the source of the Lyman continuum photons. Any source with a detectable continuum can only yield an upper-limit on  $J_{\nu 0}$ , as it will likely be dominated by local effects.

Our long slit also intercepted a [O II]  $\lambda 3727 \text{ \AA}$  emission line at  $z = 0.424$ ,  $61''.5$

East of S3, associated with a  $V = 22.8$  mag galaxy. We detect modest continuum ( $W_0[\text{O II}] = 100 \text{ \AA} \pm 10 \text{ \AA}$ ), and the redshift is confirmed with  $[\text{Ne III}] 3869 \text{ \AA}$ . The  $[\text{O II}]$  doublet is well resolved, so our resolution is better than  $221 \text{ km s}^{-1}$ .

Our search techniques failed to reveal the signature of  $\text{Ly}\alpha$  fluorescence from optically-thick clouds. A lack of  $\text{Ly}\alpha$  emission constrains the incident UV flux. In order to test the validity of our search methods and to place meaningful upper limits on  $J_{\nu 0}$ , we examined the recoverability of artificial emission lines added to our data frames. These synthetic lines simulated clouds of various sizes, and were convolved with the seeing disk and the instrumental spectral resolution. For those with shorter spatial extent, less than  $5''$ , we were able to recover 90% of the simulated spectrally unresolved lines with total  $\text{SNR} = 3$ . However, for larger artificial clouds, the recoverability was slightly worse for the same integrated  $\text{SNR}$  (but lower surface brightness). This is because slit illumination effects become more dominant on these larger scale lengths, and the spectra of the target objects introduce confusion. For  $\text{SNR} = 3$ , the recoverability falls below 60% on scales exceeding  $1'$ .

Our typical noise in a  $1 \square''$  aperture corresponds to a  $\text{Ly}\alpha$  surface brightness of  $I_{\text{Ly}\alpha(-18)} = 0.4\text{--}0.6$  ( $1 \sigma$ ). We adopt the convention  $I_{\text{Ly}\alpha(-18)} = I_{\text{Ly}\alpha} / 10^{-18} \text{ erg s}^{-1} \text{ cm}^{-2} \text{ arcsec}^{-2}$ . The quoted noise is for ‘clean’ regions of the night sky, devoid of strong lines, and the sensitivity declines slightly at the shorter wavelengths of our spectral range ( $4500 \text{ \AA} < \lambda < 6200 \text{ \AA}$ ). These limits are for a spectral extraction width of 4 pixels ( $220 \text{ km s}^{-1}$ ). This is optimal for a 1D velocity dispersion of  $\sigma_v = 30 \text{ km s}^{-1}$ , comparable to that measured for  $\text{Ly}\alpha$  forest clouds at  $z \approx 2.3$  (Kim *et al.* 1997). The line widths may in fact be greater due to coherent velocity structure (shears and bulk flows). For  $\sigma_v > 20 \text{ km s}^{-1}$ , the twin peaks of the Doppler-broadened resonant profile become resolved, and the  $\text{SNR}$  falls proportional to  $\sqrt{\sigma_v}$ . We have corrected our limits for  $A_B = 0.05$  mag of foreground Galactic extinction (Burstein & Heiles 1984). The recent COBE/IRAS dust maps of Schlegel, Finkbeiner & Davis (1998) indicate a greater extinction ( $A_B = 0.2$  mag).

Our  $3 \sigma$  upper limits on the  $\text{Ly}\alpha$  surface brightness as a function of 1D velocity dispersion and angular cloud size,  $\theta$ , projected along our  $1''$ -wide slit are:

$$I_{\text{Ly}\alpha(-18)} = (0.4 - 0.6) \left( \frac{\theta}{10''} \right)^{-1/2} \left( \frac{\sigma_v}{30 \text{ km s}^{-1}} \right)^{1/2} \quad (3 \sigma \text{ upper limit}) \quad (1)$$

for  $1'' < \theta < 60''$ ,  $2.7 < z < 4.1$  and  $\sigma_v \gtrsim 30 \text{ km s}^{-1}$ .

### 2.3. Upper Limits on $J_{\nu 0}$

We use our results to place an upper limit on  $J_{\nu 0}$  as a function of redshift and the size and velocity dispersion of the clouds. As this is derived from the limiting surface brightness attained, the constraint on the meta-galactic Lyman continuum flux is independent of  $H_0$ ,  $q_0$  and  $\Lambda_0$ , and is only subject to the  $(1+z)^4$  cosmological surface brightness dimming. The measurement of  $J_\nu$  from Ly $\alpha$  fluorescence is immune to the effects of *in situ* dust; the extra-galactic Lyman continuum photons only penetrate clouds to a depth of  $N_{\text{HI}} \approx 10^{18} \text{ cm}^{-2}$  corresponding to  $A_V \simeq 5 \times 10^{-4}$  mag for a Galactic gas-to-dust ratio. Gould & Weinberg (1996) calculate that only 4% of Ly $\alpha$  photons are absorbed as they random-walk their way out of the nebula from this depth.

An observed Ly $\alpha$  surface brightness  $I_{\text{Ly}\alpha(-18)}$  would correspond to a meta-galactic background of:

$$J_{\nu 0(-21)} = 4.76 I_{\text{Ly}\alpha(-18)} \left( \frac{0.5}{\eta_E} \right) \left( \frac{\alpha - 1}{0.73} \right) \left( \frac{1+z}{4} \right)^4 \quad (2)$$

where  $\eta_E$  is the fraction of energy absorbed from the ionizing background that is emitted in the form of Ly $\alpha$  photons (Gould & Weinberg 1996). For clouds with column depths exceeding  $N_{\text{HI}} \gtrsim 3 \times 10^{18} \text{ cm}^{-2}$ , this fraction is robust ( $\eta_E \approx 0.5$ ), but falls to  $\eta_E \approx 0.4$  for  $N_{\text{HI}} \simeq 10^{18} \text{ cm}^{-2}$ . Note that our observations constrain directly the flux of Lyman continuum photons and not  $J_{\nu 0}$  (the energy density at the Lyman edge). Conversion to  $J_{\nu 0}$  assumes a particular form of the spectrum. Specifically we adopt  $J_\nu = J_{\nu_0} (\nu/\nu_0)^{-\alpha}$  so that  $\int_{\nu_0}^{\infty} J_\nu / (h_{\text{pl}}\nu) d\nu = J_{\nu 0} / (h_{\text{pl}}\alpha)$ , where  $h_{\text{pl}}$  is Planck's constant. The HM96 spectrum has a slope  $\alpha = 1.73$ .

The greatest uncertainty on our upper limits is the size of the clouds. From a study of the foreground galaxies responsible for Mg II  $\lambda\lambda$  2796, 2803 Å QSO absorption systems at  $0.2 < z < 1.6$ , Steidel & Dickinson (1995) estimate the linear extent of LLS to be  $r_{\text{LLS}} \sim 70 h_{50}^{-1}$  kpc. For a randomly-distributed population of spherical clouds of radius  $r_{\text{LLS}}$  where the angular size of the clouds greatly exceeds the slit width ( $1'' \simeq 7 h_{50}^{-1}$  kpc at  $z \approx 3$ ), the expectation value for projected length of intersection  $\bar{D}$  along our spectroscopic slit is:

$$\bar{D} = \frac{\pi r_{\text{LLS}}}{2} \pm \left( \frac{8}{3} - \frac{\pi^2}{4} \right) r_{\text{LLS}} = (110 \pm 14) \left( \frac{r_{\text{LLS}}}{70 h_{50}^{-1} \text{ kpc}} \right) h_{50}^{-1} \text{ kpc} \quad (3)$$

This corresponds to an average angular projection of  $\theta = 15'' \pm 2''$  for  $q_0 = 0.5$  and  $\theta = 10'' \pm 1''$  for  $q_0 = 0.1$  at  $z \approx 3$ , assuming no evolution in the typical size of LLS clouds. In calculating our limits on  $J_{\nu 0}$ , we conservatively adopt an average projection of  $10''$  along the slit, consistent with the smallest likely size.

The limits we place on  $J_{\nu 0}$  as a function of redshift are depicted in Figure 1. Over



the range  $2.7 < z < 3.1$ , a wavelength region for Ly $\alpha$  where the sky spectrum is relatively featureless, our sensitivity to  $J_{\nu 0}$  is approximately flat. This is due to a combination of LRIS response, which increases towards the red, and Ly $\alpha$  line energy flux which decreases as  $(1+z)^{-4}$  through cosmological surface brightness dimming. In fact, our grating set-up (dictated by the demands of another project) was slightly red-ward of what may be most desirable for low-airmass and dark-time observations. The efficiency curve for LRIS+900 line  $\text{mm}^{-1}$  grating would suggest that  $z \approx 2.5$  is the optimal hunting ground (see Figure 1).

Our  $3\sigma$  upper limit on the meta-galactic flux over the range  $2.7 < z < 3.1$  where we are most sensitive is given by:

$$J_{\nu 0(-21)} = 2.0 \left( \frac{\theta}{10''} \right)^{-1/2} \left( \frac{\sigma_v}{30 \text{ km s}^{-1}} \right)^{1/2} \left( \frac{0.5}{\eta_E} \right) \left( \frac{\alpha - 1}{0.73} \right) \quad (3\sigma \text{ upper limit, } 2.7 < z < 3.1) \quad (4)$$

where  $\theta$  is the angular extent of the cloud, and we have assumed a resonantly-broadened line profile from a cloud with velocity dispersion  $\sigma_v$ . If the optically-thick clouds are as small as  $1''$ , the  $3\sigma$  upper limit is only  $J_{\nu 0(-21)} < 6.3$ , which is still a significant improvement over the previous limit of  $J_{\nu 0(-21)} < 200$  at  $2\sigma$  from Lowenthal *et al.* (1990). At higher redshifts, our upper limits on  $J_{\nu 0}$  are:

$$J_{\nu 0(-21)} = 3.0 \left( \frac{\theta}{10''} \right)^{-1/2} \left( \frac{\sigma_v}{30 \text{ km s}^{-1}} \right)^{1/2} \left( \frac{0.5}{\eta_E} \right) \left( \frac{\alpha - 1}{0.73} \right) \quad (3\sigma \text{ upper limit, } z \approx 3.5) \quad (5)$$

$$J_{\nu 0(-21)} = 4.0 \left( \frac{\theta}{10''} \right)^{-1/2} \left( \frac{\sigma_v}{30 \text{ km s}^{-1}} \right)^{1/2} \left( \frac{0.5}{\eta_E} \right) \left( \frac{\alpha - 1}{0.73} \right) \quad (3\sigma \text{ upper limit, } z \approx 4.0) \quad (6)$$

A concern is that we do not know *a priori* that our slit actually intercepts any optically-thick clouds. However, the incidence in QSO spectra of such clouds with column densities exceeding  $N_{\text{HI}}$  is:

$$\frac{dn}{dz} = 0.9 \left( \frac{N_{\text{HI}}}{10^{18}} \right)^{-0.5} \left( \frac{1+z}{4} \right)^{1.55} \quad (7)$$

per unit redshift (HM96). Table 1 gives the likelihood that one or more optically-thick clouds intercept our slit, where we assume a Poissonian geometric distribution of clouds with a typical projection of  $10''$ . Over the redshift interval  $2.7 < z < 3.1$  where our constraints on  $J_{\nu 0}$  are greatest, there should be on average  $\sim 1$ – $2$  such systems per arcmin surveyed. Therefore, we can reject the possibility that no  $2.7 < z < 3.1$  optically-thick absorbers lie on our  $3'$  slit at the  $> 97\%$  confidence level.

### 3. Discussion

Given the null results of our search for line emission, we consider the cosmological implications of our new upper limits on the ambient Lyman continuum background at high redshift.

#### 3.1. QSOs and the Proximity Effect

The measured decrease in the number of Ly $\alpha$ -absorbing clouds induced by the UV radiation field in the neighborhood of a QSO (the proximity effect) provides an estimate of  $J_{\nu 0}$  at high redshift, independent of  $H_0$ . A recent determination for  $1.7 < z < 3.8$  gives a mean intensity of  $J_{\nu 0(-21)} = 0.3\text{--}0.8$  (Espey 1993; Lu *et al.* 1991). These limits are a factor of 2.5–7 below our detection threshold. However, the proximity effect is subject to several systematic uncertainties;  $J_{\nu 0}$  could be underestimated if the luminosity of quasars is highly variable, or if most of the quasars with good spectra (naturally the brightest ones) are magnified by gravitational lensing, or both. From our results, the global boosting of the quasar luminosity function cannot exceed a factor of three. In addition, the number of clouds near quasars might be enhanced because of clustering. If this is not accounted for, it will lead to an underestimate of the ionizing photon flux.

The QSO luminosity function and its evolution, as derived from multi-color optical surveys, have been used to estimate the integrated QSO contribution to the UV background. A firm lower-limit over  $2 < z < 3$  is  $J_{\nu 0(-21)}^{\text{QSO}} > 0.23$  (Rauch *et al.* 1997). Accounting for the opacity of H and He associated with intervening Ly $\alpha$  clouds, Mieksin & Madau (1993) and HM96 estimate that the mean intensity of the diffuse radiation field from QSOs increases from  $J_{\nu 0(-21)}^{\text{QSO}} \approx 0.01$  at the current epoch to 0.6 at  $z = 2.6\text{--}3.0$ . This is a factor of three below our current upper limits at high redshift.

On one hand, this estimate of  $J_{\nu 0}^{\text{QSO}}$  is unknown at the 50 per cent level because of uncertainties in the evolution of the Ly $\alpha$  forest clouds (Meiksin & Madau 1993). On the other, this is an underestimate because some quasars at these redshifts may be missed through foreground dust extinction in high-column-density absorbers (Fall & Pei 1993). Our upper limit of  $J_{\nu 0(-21)} < 2.0$  indicates that at the very most, two out of three QSOs at  $z \approx 3$  are missed through absorption by foreground objects. This is at the level where we can begin to constrain the models of Fall & Pei (1993), who predict that between 10% and 70% of  $z \sim 3$  QSOs are absent from optical samples.

### 3.2. Constraints on High- $z$ Star-Forming Galaxies as the Source of Lyman Continuum Photons

It has been suggested that the young, hot OB stars in actively star-forming galaxies at high redshift may contribute significantly to the meta-galactic UV background (e.g., Songaila, Cowie & Lilly 1990). It is likely that much of the Lyman continuum radiation is absorbed by H I in the parent galaxy, i.e., the H II regions are ionization and not density bounded. Our upper limit on  $J_{\nu 0}$  at  $z \approx 3$  implies that the number of escaping Lyman continuum photons from star-forming galaxies can be a factor of no more than two greater than that contributed by quasars, assuming  $J_{\nu 0(-21)}^{\text{QSO}} \approx 0.6$  (HM96).

If we take the global star formation density from known high-redshift galaxies (e.g., Madau *et al.* 1996; Madau 1997), then we can constrain the escape fraction ( $f_{\text{esc}}$ ) of UV photons at wavelengths short-ward of the Lyman limit for these galaxies. From the HDF, the co-moving luminosity density at  $\lambda_{\text{rest}} \approx 1500 \text{ \AA}$  is  $\rho(1500 \text{ \AA}) = 2.1 \times 10^{26} h_{50} \text{ erg s}^{-1} \text{ Hz}^{-1} \text{ Mpc}^{-3}$  at  $z \approx 3$  (Dickinson 1998). For a Salpeter IMF (with  $0.1 M_{\odot} < M_* < 125 M_{\odot}$ ), this non-ionizing UV luminosity translates to an average star formation rate (SFR) per unit co-moving volume of  $\rho_{\text{SFR}}^{\text{UV}}(z \approx 3) = 0.026 h_{50} M_{\odot} \text{ yr}^{-1} \text{ Mpc}^{-3}$ , assuming no obscuration. However, from recent near-infrared observations of nebular emission lines, Pettini *et al.* (1997, 1998) estimate that the UV continuum at  $z \approx 3$  is extinguished by  $A_{1500} \approx 1\text{--}2$  mag, implying that the total star formation rates are a factor of 3–6 higher. This is broadly consistent with the recent HDF sub-mm detections by SCUBA/JCMT (Hughes *et al.* 1998) corresponding to  $\rho_{\text{SFR}}^{\text{FIR}} = 0.1 h_{50} M_{\odot} \text{ yr}^{-1} \text{ Mpc}^{-3}$  at  $z \approx 3$ . Applying the Calzetti (1997) extinction curve derived from local star-burst galaxies to the  $z \approx 3$  population yields a similar rest-UV extinction (a factor of 2–6; Calzetti 1998).

A constant star formation rate of  $1 M_{\odot} \text{ yr}^{-1}$  will produce  $1.44 \times 10^{53} \text{ s}^{-1}$  Lyman continuum photons, from the most recent version of the spectral evolutionary code of Bruzual & Charlot (1993) with the same Salpeter IMF. Hence, the  $z \approx 3$  galaxies produce Lyman continuum photons at a volume-averaged rate of:

$$\dot{n}_{\text{LyC}} = 2.45 \times 10^{-20} \left( \frac{10^{0.4A_{1500}}}{3} \right) \left( \frac{1+z}{4} \right)^3 h_{50} \text{ photons s}^{-1} \text{ cm}^{-3} \quad (8)$$

where  $\dot{n}_{\text{LyC}}$  is in physical rather than co-moving co-ordinates. The mean free path of a Lyman continuum photon,  $\Delta l$ , is inferred from Madau (1992), who shows that unit optical depth is achieved for  $\Delta z \approx 0.2$  at  $z = 3$ , corresponding to a physical length of  $\Delta l \approx 40 h_{50}^{-1} \text{ Mpc}$  (i.e., the ionizing flux is largely local, and evolutionary effects can be neglected as Lyman-continuum photons from galaxies at higher redshifts are either severely

absorbed or redshifted to energies below the Lyman edge). Therefore, the contribution of star-forming galaxies to  $J_{\nu 0}$  is given by:

$$J_{\nu 0}^{\text{SFR}} = f_{\text{esc}} \frac{h_{\text{pl}} \alpha}{4\pi} \Delta l \dot{n}_{\text{LyC}} \quad (9)$$

for an ionizing spectrum of the form  $J_{\nu} = J_{\nu 0}(\nu/\nu_0)^{-\alpha}$ , which can be expressed as:

$$J_{\nu 0(-21)}^{\text{SFR}} = 0.28 \left( \frac{f_{\text{esc}}}{10\%} \right) \left( \frac{\alpha}{1.73} \right) \left( \frac{\Delta l}{40 h_{50}^{-1} \text{Mpc}} \right) \left( \frac{\rho_{\text{SFR}}^{\text{UV}}}{0.026 h_{50}} \right) \left( \frac{10^{0.4A_{1500}}}{3} \right) \left( \frac{1+z}{4} \right)^3 \quad (10)$$

Therefore, the dust-corrected SFR per unit co-moving volume at  $z \approx 3$  is equivalent to  $J_{\nu 0(-21)} = (3 - 6) f_{\text{esc}}$ , if the rest-UV is extinguished by factors of 6–3. Hence, our  $3 \sigma$  limit of  $J_{\nu 0(-21)} = 2.0$  constrains  $f_{\text{esc}} < 25\% - 50\%$ , assuming QSOs contribute  $J_{\nu 0(-21)}^{\text{QSO}} = 0.6$  (HM96). However, Meurer *et al.* (1997) argue that *in situ* dust obscuration leads to a much greater underestimate of the integrated star formation rate, and that the rest-UV extinction correction should be a factor of  $\approx 15$  rather than 3–6. If this is so, our constraint is significantly tighter ( $f_{\text{esc}} < 10\%$  at  $z \approx 3$ ), comparable to but still somewhat above the best limits on the Lyman continuum escape fraction from galaxies today ( $f_{\text{esc}} < 1\%$ , Deharveng *et al.* 1997).

### 3.3. Gunn-Peterson Constraint on the Diffuse IGM

The absence of an absorption trough on the blue side of the Ly $\alpha$  emission line in the spectra of high-redshift QSOs represents the best limit on the density of a neutral, smoothly-distributed IGM (Gunn & Peterson 1965; Scheuer 1965). A measurement of the ionizing meta-galactic flux, when combined with limits on the baryon density from primordial nucleosynthesis and the Gunn-Peterson optical depth (Jenkins & Ostriker 1991; Giallongo, Cristiani & Trevese 1992) measures what fraction of gas has collapsed into galaxies and discrete clouds. Our upper limit on  $J_{\nu 0}$  requires that baryonic matter in the diffuse IGM comprises  $\Omega_{\text{IGM}} < 0.016 h_{50}^{-3} \Omega_{\text{crit}}$  of the closure density at  $z \approx 3$  (from Equation 2 of Songaila, Cowie & Lilly 1990). We assume the mean optical depth of the IGM is  $\tau_{z \approx 3} < 0.02$  (Steidel & Sargent 1987). From standard Big Bang nucleosynthesis (Walker *et al.* 1991), our results imply that the fraction of baryons residing in the diffuse IGM at  $z \approx 3$  is at most  $60\% / h_{100}$  (where  $h_{100} = H_0 / 100 \text{ km s}^{-1} \text{ Mpc}^{-1}$ ), i.e., no constraint for low values of  $H_0$ . We are undertaking deeper integrations which should improve this upper limit by a factor of three.

### 3.4. Decaying Relativistic Neutrinos and the Meta-Galactic UV Background

The recent Super-Kamiokande detection of neutrino oscillation (Fukuda *et al.* 1998), although providing only a mass difference between neutrino flavors rather than an absolute measurement of mass, has rekindled interest in Hot Dark Matter (HDM). We can use our upper limits on  $J_{\nu 0}$  to constrain any relic decaying neutrino flux (e.g., Sciama 1990). According to this theory, relativistic neutrinos make up the bulk of the critical matter density ( $\Omega_\nu \approx 0.9 \Omega_{\text{crit}}$ ), and their decay photons can ionize hydrogen (i.e.,  $E_\gamma > 13.6$  eV) but not helium. Adopting the values from Sciama (1995, 1998) for the decay photon energy ( $E_\gamma \lesssim 13.8$  eV), the neutrino lifetime ( $\tau_\nu \approx 2 \times 10^{23}$  s) and number density at the current epoch ( $N_\nu = 112.6 \text{ cm}^{-3}$ ) would result in a UV flux at  $z \approx 3$  equivalent to  $J_{\nu 0(-21)} = 4.5$  (Figure 1). This would correspond to a  $6 \sigma$  signal in our spectrum over  $2.7 < z < 3.3$ . Our failure to detect such Ly $\alpha$  emission rules out with high confidence a  $\Omega_M = 1$  cosmology in which the relativistic decaying neutrinos of Sciama (1998) form the bulk of dark matter. Furthermore, in a Mixed Dark Matter (MDM) scenario, an HDM component in the form of  $E_\gamma = 13.8$  eV Sciama neutrinos can comprise at most  $\Omega_\nu < 0.4 \Omega_{\text{crit}}$ .

Our observations constrain the combination of parameters  $(E_\gamma - 13.6 \text{ eV}) / (\tau_\nu H_0)$ , the excess photon energy above the Lyman limit available for photo-ionization. If the neutrinos do account for most of the critical matter density in a flat Universe (i.e.,  $\Omega_\nu \gtrsim 0.9 \Omega_{\text{crit}}$ ,  $\Omega_{\text{baryon}} \lesssim 0.1 \Omega_{\text{crit}}$ ), then

$$(E_\gamma - 13.6 \text{ eV}) = 0.08 h_{50} \times \frac{\tau_\nu}{2 \times 10^{23} \text{ s}} \text{ eV} \quad (3 \sigma \text{ upper limit}) \quad (11)$$

Therefore, the energy of the decay photons can be at most only 0.6 per cent above the ionization potential of H I, which would require much fine-tuning.

## 4. Conclusions & Future Work

Our moderate-dispersion long-slit spectroscopy with LRIS/Keck has placed a  $3 \sigma$  upper limit on the ambient UV background at  $z \approx 3$  equivalent to a flux at the Lyman limit of  $J_{\nu 0(-21)} < 2.0$ , assuming optically-thick clouds with dimensions  $\approx 10''$ . We anticipate even greater sensitivity in the blue for observations at lower air mass and unaffected by cirrus. Although this direct limit is almost two orders of magnitude lower than any previously published, it is still a factor of three above the expected contribution of known QSOs at these epochs. However, it does enable us to say that the completeness of optical QSO catalogs is better than 30%, and that the contribution to  $J_{\nu 0}(z \approx 3)$  from star-forming galaxies cannot exceed twice that from known quasars. We constrain the escape fraction of Lyman

continuum photons from star-forming galaxies at these redshifts to be  $f_{\text{esc}} < 10\%–50\%$  (assuming extinction corrections of 15–3 at  $\lambda_{\text{rest}} \approx 1500 \text{ \AA}$ ). Although our relatively short (5400 s) integration in this pilot study is insufficient to reach the lower limit on the quasar contribution to  $J_{\nu 0}$ , we are able to exclude the possibility that relic neutrinos comprise the bulk of dark matter, as we would detect Ly $\alpha$  fluorescence from the flux of ionizing decay photons.

The size of optically-thick QSO absorption systems is largely unconstrained (§2.3), and their morphology is entirely unknown because quasar sight-lines yield only one-dimensional information. Some work has been done using two lines-of-sight provided, for example, by a pair of lensed quasar images (e.g., Dinshaw *et al.* 1994). The single example of multiple sight-lines to a damped system indicates a size greater than  $16 h_{50}^{-1} \text{ kpc}$  (Briggs *et al.* 1989). Without strong constraints on the sizes of the high-column-density systems, it is impossible to differentiate between the scenario where outer galactic halos are directly responsible for the absorption or whether the culprit is more extended diffuse gas. This may be associated with a cluster, possibly with a fragmented, filamentary topology (as suggested by recent SPH simulations, e.g., Katz *et al.* 1996). A detection of fluorescent Ly $\alpha$  would reveal the size and morphology of the optically-thick clouds, which is a primary clue to understanding their origin and relation to the galaxies which are forming at these epochs.

The phenomenal light-grasp of Keck plus the new insights afforded by Gould & Weinberg (1996) make it possible to design an experiment with an extremely high likelihood of detecting fluorescent Ly $\alpha$  emission from high-column Lyman limit absorbers. This will enable the first direct measurement of the size of these high-redshift H I clouds, and the determination of  $J_{\nu 0}$  at  $z \approx 2.5–3$ . This initial study has shown that, for a dark-time integration of  $\sim 20$  hours in good conditions, the sensitivity of LRIS/Keck should be sufficient to detect the Lyman continuum background at  $> 5 \sigma$ , even if the meta-galactic flux has no major contribution other than the known high-redshift quasars. We are embarking on an extensive program of LRIS/Keck observations to obtain long-slit spectra of several hours. By using a filter of width  $\Delta\lambda/\lambda \approx 10\%$ , we can obtain several parallel long-slits on the same spectrogram, thereby covering a large solid angle while concentrating on those redshifts ( $z \approx 2.5$ ) where our sensitivity to  $J_{\nu}$  is greatest (Figure 2). For the first time we will set strict quantitative limits on the inventory of sources of UV radiation at high redshift.

We are indebted to Hy Spinrad and Steve Warren for allowing us to use their spectroscopic data for this blank-sky search. Our thanks to Daniel Stern, Arjun Dey and Adam Stanford for their help during the observing run. The software for rejecting cosmic ray strikes was written by Mark Dickinson. Douglas Finkbeiner kindly provided us

with the extinction from the COBE/IRAS maps. We gratefully acknowledge invaluable discussions with Joe Silk, Nick Gnedin, Marc Davis, Neal Katz, Mark Lacy & Chuck Steidel. Palle Møller graciously provided us with imaging of this field. Our thanks to Daniel Stern, Michael Liu and Leonidas Moustakas for comments on an early version of this manuscript. We appreciate the constructive suggestions of our referee, Andrew Gould. The data presented herein were obtained at the W. M. Keck Observatory, which is operated as a scientific partnership among the California Institute of Technology, the University of California and the National Aeronautics and Space Administration. The Observatory was made possible by the generous financial support of the W. M. Keck Foundation. We received excellent support while observing at Keck, and we are grateful to Bob Goodrich, Fred Chaffee, Tom Bida, Terry Stickel & David Sprayberry. A.J.B. acknowledges a NICMOS postdoctoral research fellowship. F.R.M. would like to acknowledge support from the HST NASA grant #AR-07523.01. J.R.G. is supported by the Packard Foundation.

## REFERENCES

- Binette, L., Wang, J. C. L., Zuo, L., & Magris C., G. 1993, *AJ*, 105, 797
- Bland-Hawthorn, J., Freeman K. C., & Quinn P. J. 1997, *ApJ*, 490, 143
- Briggs, F. H., Wolfe, A. M., Liszt, H. S., Davis, M. M., & Turner, K. L. 1989, *ApJ*, 341, 650
- Bruzual A., G., & Charlot, S. 1993, *ApJ*, 405, 538
- Bunker, A. J., *et al.* 1998, in preparation
- Burstein, D., & Heiles, C. 1984, *ApJS*, 54, 33
- Calzetti, D. 1997, *AJ*, 113, 162
- Calzetti, D. 1998, in “XXIIIrd Recontres de Moriond on Dwarf Galaxies and Cosmology”, eds., Thuan, T.X., Balkowski, C., Cayatte, V., & Tran Thanh Van, T. (astro-ph/9806083)
- Charlot, S., & Fall, S. M. 1993, *ApJ*, 415, 580
- Deharveng, J. -M., Faiesse, S., Milliard, B., & Le Brun, V. 1997, *A&A*, 325, 1259
- Dickinson, M. E. 1998, in “The Hubble Deep Field”, eds. Livio, M., Fall, S. M., Madau, P. STScI Symposium Series (astro-ph/9802064)
- Dinshaw, N., Impey, C., Foltz, C., Weymann, R., & Chaffee, F. 1994, *ApJ*, 437, 87
- Dove, J. B. & Shull, J. M. 1994, *ApJ*, 423, 196
- Espey, B. R. 1993, *ApJ*, 411, 59
- Fall, S. M., & Pei, Y. C. 1993, *ApJ*, 402, 479

- Ferrara, A., & Field, G. B. 1994, *ApJ*, 423, 665
- Fukuda, Y., Hayakawa, T., Ichihara, E., *et al.* 1998, *Phys. Rev. Lett.*
- Giallongo, E., Cristiani, S., & Trevese, D. 1992, *ApJ*, 398, 9
- Giallongo, E., D’Odorico, S., Fontana, A., McMahon, R. G., Savaglio, S., Cristiani, S., Molaro, P., & Trevese, D. 1994, *ApJ*, 425 1
- Gould, A. & Weinberg, D. H. 1996, *ApJ*, 468, 462
- Gunn, J. E., Peterson, B. A. 1965, *ApJ*, 142 1633
- Haardt, F. & Madau, P. (HM96) 1996, *ApJ*, 461, 20
- Hogan, C. J., & Weymann, R. J. 1987, *MNRAS*, 225 1P
- Hughes, D., Serjeant, S., Dunlop, J., *et al.* 1998, *Nature*, in press (astro-ph/9806297)
- Jenkins, E. B. & Ostriker, J. P. 1991, *ApJ*, 376, 33
- Katz, N., Weinberg, D. H., Hernquist, L., & Miralda-Escudé, J. 1996, *ApJ*, 457, 57
- Kim, T.-S., Hu, E. M., Cowie, L. L., & Songaila, A. 1997, *AJ*, 114, 1
- Lanzetta, K. M., Wolfe, A. M., & Turnshek, D. A. 1995, *ApJ*, 440, 435
- Lowenthal, J. D., Hogan, C. J., Leach, R. W., Schmidt, G. D., & Foltz, C. B. 1990, *ApJ*, 357, 3
- Lu, L., Wolfe, A. M., Turnshek, D. A. 1991, *ApJ*, 367, 19
- Madau, P. 1992, *ApJ*, 389, 1
- Madau, P., Fergusson, H. C., Dickinson, M. E., Giavalisco, M., Steidel, C. C., & Fruchter, A. 1996, *MNRAS*, 283, 1388
- Madau, P. 1997, in “The Hubble Deep Field”, eds. Livio, M., Fall, S. M., Madau, P. *STScI Symposium Series* (astro-ph/9709147)
- Maloney, P. 1993, *ApJ*, 414, 41
- Martínez-González, J. I., González-Serrano, L., Cayón, L., Sanz, J. L., & Martín-Mirons, J. M. 1995, *A&A*, 303, 379
- Massey, P. & Gronwall, C. 1990, *ApJ*, 358, 344
- Massey, P., Strobel, K., Barnes, J. V. & Anderson, E. 1988, *ApJ*, 328, 315
- Meiksin, A. & Madau, P. 1993, *ApJ*, 412, 34
- Meurer, G. B., Heckman, T. M., Lehnert, M. D., Leitherer, C., & Lowenthal, J. D. 1997, *AJ*, 114, 54
- Møller P., & Warren S. J. 1993, *A&A*, 270, 43



- Møller P., & Warren S. J. 1998, MNRAS, in press (astro-ph/9804205)
- Oke, J. B., Cohen, J. G., Carr, M., Cromer, J., Dingizian, A., Harris, F. H., Labrecque, S., Lucinio, R., Schall, W., Epps H. & Miller, J. 1995, PASP, 107, 375
- Pettini, M., Steidel, C. C., Adelberger, K. L., Kellogg, M., Dickinson, M., & Giavalisco, M. 1997 (astro-ph/9708117)
- Pettini, M., Kellogg, M., Steidel, C. C., Dickinson, M., Adelberger, K. L., & Giavalisco, M. 1998, ApJ, in press (astro-ph/9806219)
- Rauch, M., Miralda-Escudé, J., Sargent, W. L. W., *et al.* 1997, ApJ, 489, 7
- Scheuer, P. A. G., 1965, Nature, 207, 963
- Schlegel, D. J., Finkbeiner, D. P., & Davis, M. 1998, ApJ, 500, 525
- Sciama, D. W. 1990, Phys. Rev. Lett., 65, 2839
- Sciama, D. W. 1995, ApJ, 448, 667
- Sciama, D. W. 1998, A&A, 335, 12
- Songaila, A., Cowie, L. L., & Lilly, S. J. 1990, ApJ, 348, 371
- Steidel, C. C., Sargent, W. L. W. 1987, ApJ, 313, 171
- Steidel, C. C. 1990, ApJS, 74, 37
- Steidel, C. C., & Dickinson, M. 1995, in “Wide Field Spectroscopy and the Distant Universe”, eds. Maddox, S. J., & Aragón-Salamanca, A. (Singapore World Sci.), p349
- Steidel C. C., Giavalisco M., Pettini M., Dickinson M. E., & Adelberger K. L. 1996, ApJ, 462, 17
- Stengler-Larrea E., Boksenberg, A., Steidel, C. C., *et al.* 1995, ApJ, 444, 64
- Warren, S. J., & Møller, P. 1996, A&A, 311, 25
- Walker, T. P., Steigman, G., Schramm, D. N., Olive, K. A., & Kang, H. S. 1991, ApJ, 376, 51
- Williams, R. E., Blacker, B., Dickinson, M., Dixon, W. V. D., Ferguson, H. C., Fruchter, A. S., Giavalisco, M., Gilliland, R. L., Heyer, I., Katsanis, R., Levay, Z., Lucas, R. A., Mcelroy, D. B., Petro, L., & Postman, M. 1996, AJ, 112, 1335

Table 1. Upper Limits and Detection Statistics

	$N_{\text{HI}} / \text{cm}^{-2}$	
	$> 10^{18}$	$> 3 \times 10^{18}$
$\eta_E$	0.4	0.5
$J_{\nu 0(-21)}$ $3 \sigma$ limit	2.5	2.0
# of clouds / arcmin	2.0	1.2
$P(n_{\text{cloud}} \geq 1)$	99.8%	97.3%

Note. — For the redshift interval  $2.7 < z < 3.1$  where our limits on  $J_{\nu 0}$  are most stringent.

Fig. 1.— Our  $3\sigma$  upper-limits on the flux density at the Lyman edge,  $J_{\nu 0(-21)} = J_{\nu 0} / 10^{-21} \text{ erg s}^{-1} \text{ cm}^{-2} \text{ Hz}^{-1} \text{ sr}^{-1}$ , as a function of redshift (solid line). We assume a meta-galactic UV spectrum of the form  $J(\nu) \propto \nu^{-\alpha}$  with  $\alpha = 1.73$  (HM96). The right axis shows the flux of Lyman continuum photons ( $\int_{\nu_0}^{\infty} J_{\nu} / h_{\text{pl}} \nu d\nu$ ), which is measured independent of  $\alpha$ . The region above the heavy solid curve is excluded at the 90% confidence level. Spikes of reduced sensitivity occur at redshifts where Ly $\alpha$  coincides with the sky lines in our 1.5 hour spectrogram. These limits assume that a long 1'' slit covers  $\sim 10 \square''$  of an optically-thick cloud ( $N_{\text{HI}} \gtrsim 3 \times 10^{18} \text{ cm}^{-2}$ ) and that the cloud velocity dispersion is  $\sigma_v \lesssim 30 \text{ km s}^{-1}$ . Also shown are the previous  $3\sigma$  upper-limits from the INT (Martínez-González 1995) and the MMT (Lowenthal *et al.* 1990), converted to the same assumed projected cloud size. We plot our anticipated sensitivity for a 20 hour exposure with LRIS+900 line  $\text{mm}^{-1}$  at low airmass in dark time (dotted curved). The shaded region is the lower-limit on  $J_{\nu 0}$  from the proximity effect (Espey 1993). The estimated contribution to  $J_{\nu 0}$  from the luminosity function of known high- $z$  QSOs is also shown as the dashed line (HM96). The equivalent Lyman continuum flux from decaying relic neutrinos is plotted as a dot-dash line, adopting the parameters of Sciama (1998) and assuming these neutrinos form the bulk of the dark matter in an  $\Omega_{\text{M}} = 1$  Universe. Such a scenario is strongly ruled out by the null results of our survey.

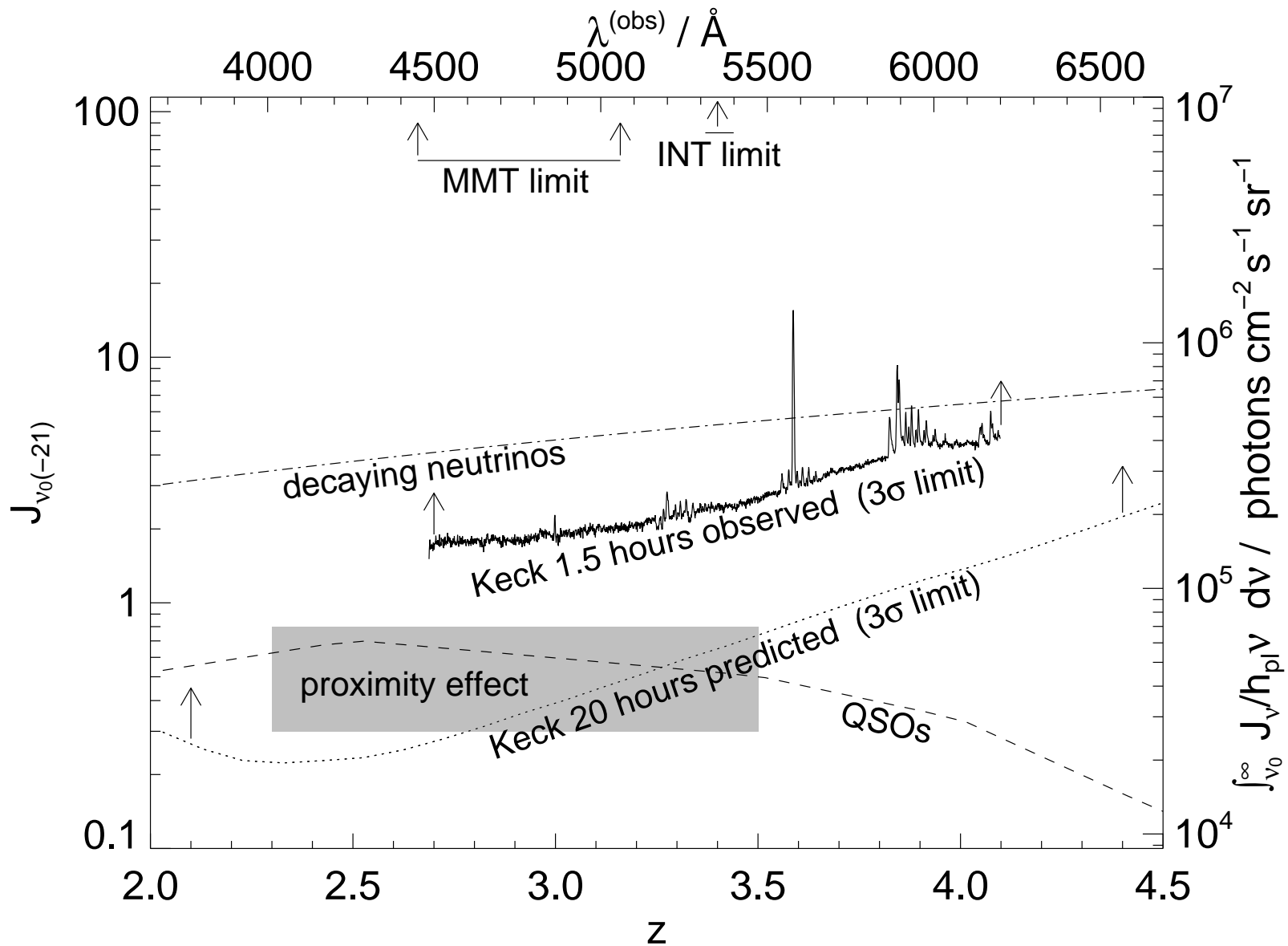


Fig. 2.— The number of sources intercepted above a given SNR threshold ( $\text{SNR} > 5$ ) in a 10–20 hour spectrum as a function of the number of slits. We perform this calculation for the LRIS spectrograph on Keck with the 900 line  $\text{mm}^{-1}$  grating set to  $\lambda_{\text{cent}} = 4047 \text{ \AA}$ . Given the redshift distribution of Ly $\alpha$  absorbers and our limits on  $J_{\nu 0}$  as a function of wavelength (Figure 1), we are most sensitive to clouds over a relatively limited range of redshifts. This means that pixels in the detector array are better used in the spatial dimension rather than the spectral dimension. Having multiple slits trades wavelength range for area covered. Since LRIS is equipped with a slit mask mechanism we can insert several parallel long slits of length  $\approx 7'$  at the focal plane. A custom narrow band filter ( $\Delta\lambda/\lambda \approx 10\%$ ) would be used to prevent spectral overlap. This figure shows the increase in the efficiency by using this multi-slit Ly $\alpha$  search technique. We conservatively assume that the number of clouds per unit redshift interval scales as  $(1+z)$ , which is correct for damped Lyman alpha systems (Lanzetta, Wolfe & Turnshek 1995). For lower-column systems,  $dn/dz \propto (1+z)^\gamma$ , where  $\gamma \approx 1.5$  (Stengler-Larrea *et al.* 1995). Adoption of this steeper distribution would favor a multi-slit search even more.

